

# Why are nonlinear fits to data so challenging?

Mark K. Transtrum, Benjamin B. Machta, and James P. Sethna

Laboratory of Atomic and Solid State Physics, Cornell University, Ithaca, New York 14853, USA\*

Fitting model parameters to experimental data is a common yet often challenging task, especially if the model contains many parameters. Typically, algorithms get lost in regions of parameter space in which the model is unresponsive to changes in parameters, and one is left to make adjustments by hand. We explain this difficulty by interpreting the fitting process as a generalized interpolation procedure. By considering the manifold of all model predictions in data space, we find that cross sections have a hierarchy of widths and are typically very narrow. Algorithms become stuck as they move near the boundaries. We observe that the model manifold, in addition to being tightly bounded, has low extrinsic curvature, leading to the use of geodesics in the fitting process. We improve the convergence of the Levenberg-Marquardt algorithm by adding the geodesic acceleration to the usual Levenberg-Marquardt step.

The estimation of model parameters from experimental data is astonishingly challenging. A nonlinear model with tens of parameters, fit (say) by least-squares to experimental data, often takes weeks of hand-fiddling before a qualitatively reasonable agreement can be found; even then, the parameters cannot usually be reliably extracted from the data. Both minimization algorithms and algorithms like Levenberg-Marquardt that are designed for least-squares fits routinely will get lost in parameter space. This becomes a serious obstacle to progress when one is unsure of the validity or quality of the model, e.g. in systems biology where one wants to automatically generate and explore a variety of alternative models.

Here we use differential geometry to explain why fits are so hard. We first explore the structure of the *model manifold*  $\mathcal{M}$ , the manifold of predictions embedded in the space of data,  $D$ , and find that it is typically bounded, with cross sections having a hierarchy of widths, so that the overall structure is similar to that of a long, thin ribbon. We explain this hierarchy by viewing the fitting process as a generalized interpolation procedure with few effective model degrees of freedom. We interpret the difficulty in fitting to be due to algorithms getting stuck near the boundary of  $\mathcal{M}$ , where the model is unresponsive to variations in the parameters. We then discuss how geometry motivates algorithms to alleviate the difficulties.

A typical nonlinear least squares problem fits a model  $Y_m(\theta)$  with  $N$  parameters  $\theta$  to  $M$  experimental data points  $y_m$ . We define the model manifold,  $\mathcal{M}$ , as the parametrized  $N$ -dimensional surface  $\vec{Y}(\theta)$  embedded in Euclidean data space,  $D = \mathbb{R}^M$ . The best fit to the experiment is given by the point on  $\mathcal{M}$  with Euclidean distance closest to the data, minimizing the cost  $C = \frac{1}{2} (\vec{Y}(\theta) - \vec{y})^2$ . The Euclidean metric of data space (with distance between models given by the change in residuals  $\vec{Y}(\theta) - \vec{y}$ ) induces a metric on the manifold,  $g_{\mu\nu} = \partial_\mu \vec{Y} \cdot \partial_\nu \vec{Y} = (J^T J)_{\mu\nu}$ , where  $J_{m\mu} = \frac{\partial}{\partial \theta_\mu} Y_m$ . (Gen-

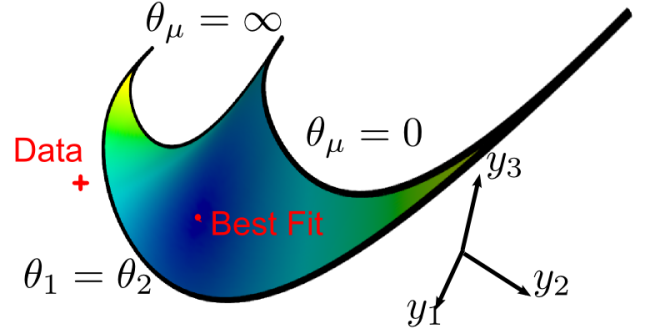


Figure 1: The model manifold for the two-exponential problem, with  $y_i$  evaluated at  $t = 1/3, 1$ , and  $3$ . Boundaries exist when  $\theta_\mu = 0, \infty$  and when  $\theta_1 = \theta_2$ .

eralizing to weighted least squares is a straightforward rescaling of each Cartesian axis in data space.) We note that the metric is the approximate Hessian, or second derivative matrix, of the cost  $C$ , assuming that the point exactly reproduces the data. The model manifold for the two exponential model  $Y(t, \theta) = f_\theta(t) = e^{-\theta_1 t} + e^{-\theta_2 t}$  sampled at three time points is given in Fig. 1 and demonstrates the ribbon-like nature of  $\mathcal{M}$ . By generalizing this model to more parameters and data points, the higher-dimensional surface becomes increasingly narrow. If the data is continuous on  $(-\infty, \infty)$  in log-time, the metric here is given simply by  $g_{\mu\nu} = \frac{1}{(\theta_\mu + \theta_\nu)^2}$ .

To understand the hierarchy of widths, consider the special case of analytic models,  $f(t, \theta)$ , of a single independent variable (time) where the data points are  $Y_m = f(t_m)$ . Let  $R$  be the typical time scale over which the model behavior changes, so that the  $n^{\text{th}}$  term of the Taylor series  $f^{(n)}(t)/n! \lesssim R^{-n}$  (roughly the radius of convergence). If the function is sampled at  $n$  time point  $(t_1, t_2, \dots, t_n)$  within this time scale, the Taylor series may be approximated by the unique polynomial of degree  $n - 1$ ,  $P_{n-1}(t)$  passing through these points. At a new point,  $t_0$ , the discrepancy between the interpolation

\*Electronic address: mkt26@cornell.edu

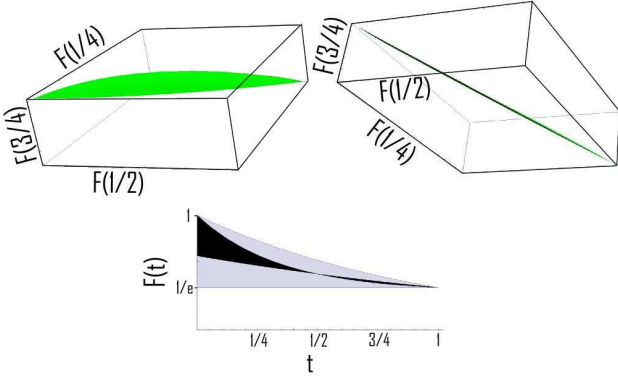


Figure 2: Top: Two views of the cross section of the model manifold for an *infinite* sum of exponentials  $F_{A,\theta}(t) = \sum_n A_n \exp(-\theta_n t)$  with  $A_n \geq 0$ , given by fixing  $F(0) = 1$  and  $F(1) = 1/e$ . Bottom: The range of allowed fits (grey) is strongly reduced by fixing the output at  $t = 1/2$  to the midpoint of its range (black).

and the function is given by

$$f(t_0) - P_{n-1}(t_0) = \frac{\omega_n(t_0)f^{(n)}(\xi)}{n!}, \quad (1)$$

where  $\xi$  lies somewhere in the interval containing  $t_0, t_1, \dots, t_n$  [1]. The polynomial  $\omega_n(t)$  has roots at each of the interpolating points  $\omega_n(t) = (t-t_1)(t-t_2)\dots(t-t_n)$ . The possible error of the interpolation function is simply the allowed range of behavior,  $\Delta f_n$ , of the model at  $t_0$  after constraining the nearby  $n$  data points (taking cross sections).

Consider the ratio of successive cross sections,  $\frac{\Delta f_{n+1}}{\Delta f_n} = (t - t_{n+1})(n+1) \frac{f^{n+1}(\xi)}{f^n(\xi')}$ . If  $n$  is sufficiently large, then  $(n+1) \frac{f^{n+1}(\xi)}{f^n(\xi')} \approx \frac{1}{R}$ ; therefore, we find that  $\frac{\Delta f_{n+1}}{\Delta f_n} \approx \frac{t-t_{n+1}}{R} < 1$  by the ratio test. Each cross section is thinner than the last by a roughly constant factor, yielding the observed hierarchy of widths.

Because of the increasingly narrow cross-sections of  $\mathcal{M}$ , there are necessarily directions in parameter space to which the model behavior is very insensitive. Previously, an analysis of the Hessian,  $J^T J$ , revealed eigenvalues that may have ranges greater than  $10^6$ , as in Fig. 3, a phenomenon known as sloppiness [2, 3, 4, 5]. Eigendirections corresponding to the smallest eigenvalues are known as sloppy directions, and model behavior is thus a thousand or more times less sensitive in these directions than in the well-constrained stiff eigendirections.

To understand the relation between the local eigendirections of the Hessian and the cross sectional widths, we now consider the linear sloppy model of fitting polynomials,  $f(t, \theta) = \sum_\mu \theta_\mu t^\mu$ . In the case of continuous data on  $(0, 1)$ , the Jacobian is given by  $J_\mu(t) = t^\mu$ , and the metric  $(J^T J)_{\mu\nu} = \int_0^1 t^\mu t^\nu dt = \frac{1}{\mu+\nu+1}$  is the famously ill-conditioned Hilbert matrix, whose eigenvalues are given in Fig. 3b. We focus on the parameter values within the

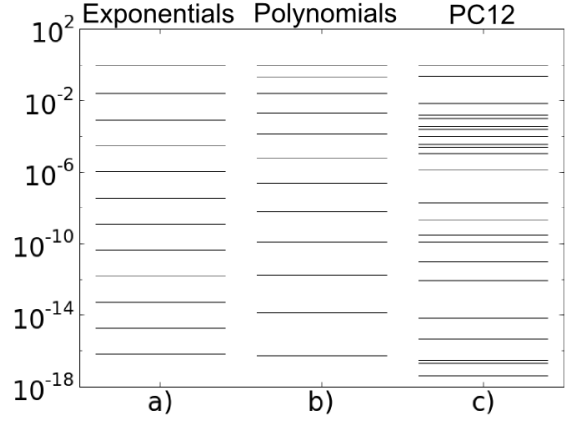


Figure 3: The eigenvalues of the Hessian of sloppy models span many order of magnitude. Examples of sloppy models include a) the sum of 12 logarithmically spaced exponential rates [3],  $g_{\mu\nu} = \frac{1}{(\theta_\mu + \theta_\nu)^2}$ , b) polynomials [3],  $g_{\mu\nu} = \frac{1}{\mu+\nu+1}$ , or c) a model of epidermal growth factor in rat pheochromocytoma (PC12) cells from systems biology [2].

unit hyper-sphere in parameter space,  $\sum_\mu \theta_\mu^2 \leq 1$ , corresponding roughly to a radius of convergence of 1, and consider the image of this domain under the mapping to data space. Without some such restriction, one can always fit any data perfectly with a sufficiently large polynomial, a consequence of the linearity of the model. In contrast, for most nonlinear models, Eq. 1 places stringent bounds on the interpolation. By restricting ourselves to the unit hyper-sphere we are imitating the nonlinear behavior by ensuring that higher derivatives of  $f(t)$  become vanishingly small and that the Taylor series converges.

Since the model is linear, it takes the form  $Y_m = \sum_\mu J_{m\mu} \theta_\mu$ , where the Jacobian (for discrete data) is a Vandermonde matrix,  $J_{m\mu} = t_m^\mu$ . A singular value decomposition of the Jacobian,  $J = U \Sigma V^T$ , where  $U$  and  $V$  are unitary matrices and  $\Sigma$  is diagonal, helps to understand the mapping. Under this decomposition,  $J^T J = V \Sigma^2 V^T$ , so that columns of  $V$  are eigenvectors of the metric whose eigenvalue is the square of the singular value. Therefore, the eigenvectors  $V_\mu$  are stretched by their corresponding singular values and mapped into the directions of  $U_\mu$  in data space. The image of the hyper-sphere in parameter space is a hyper-ellipsoid in data space with a hierarchy of lengths for each principle axis. The stiff eigenvectors are mapped into the long axes, while the sloppy eigenvectors are mapped into the thin axes. The overall image is that of a long, thin hyper-ribbon.

The recognition that sloppiness is ubiquitous can now be reinterpreted: multiparameter models are a kind of high-dimensional analytic interpolation scheme, and sloppiness results whenever multiple data points reside within some generalized radius of convergence. When this is the case, the data points are highly correlated and the model has few effective degrees of freedom. When-

ever there are many model parameters for each model degree of freedom there will be a hierarchy of widths and the model will be sloppy.

Our geometric interpretation explains a number of observations about sloppy models. First, it has been stated previously [5] that fitting sloppy models to experimental data is able to constrain the outcomes of new experiments in spite of large uncertainties in parameter values. Because the fitting process is an interpolation scheme, only a few stiff parameter combinations need to be tuned to fit most of the data, since only a few data points constrain the predictions at other times. The remaining sloppy parameter combinations control the interpolated values, which are restricted by the analyticity of the model.

Another unexpected finding is that the extrinsic curvatures of the model manifold tend to be quite small. The manifold is trivially flat if there are equal numbers parameters and data points,  $N = M$ . In this case the manifold is embedded in an Euclidean space of equal dimension, and is therefore Euclidean itself. In general, most of the data points are interpolations that supply little new information. Points within  $R$  have strongly correlated responses to parameters, leading to a smaller number of effective data points and producing a flat manifold. Although the manifold is nearly flat, the model is often highly nonlinear. When this is the case, the nonlinearities are due to parameter-effects curvature [6], which are typically the dominant nonlinearities in sloppy models.

Considering the motion of geodesic on the model manifold, we find that they are nearly straight lines due to the low extrinsic curvature. We use geodesics to construct new coordinates  $\gamma^\mu = \gamma^\mu(\theta)$  that generalize Riemann normal coordinates [7]. The coordinates are polar with the origin at the best fit and angular coordinates defining the direction of a geodesic. The radial coordinate is given by the distance along the geodesic. Since geodesics are nearly straight lines in data space on  $\mathcal{M}$ , we find that cost contours in these coordinates are nearly quadratic and isotropic around the best fit, as explicitly computed in Fig. 4. Sloppy nonlinear models locally look like linear models with badly chosen parameters, well beyond the harmonic approximation (the model manifold is extrinsically nearly flat), but globally they have exceptional constraints in their range of predictions (the boundaries of the ribbon-like model manifold).

Can geodesics inspire algorithms that lead efficiently to the best fit? If we attempt to integrate the geodesic equation with a single Euler step, we reproduce the Gauss-Newton step, which in our notation is  $\delta\theta^\mu = -g^{\mu\nu}\nabla_\nu C$ . In practice, however, this method is very ineffective at finding good fits. This is due to the enormous eigenvalues in the inverse metric  $g^{\mu\nu}$  due to sloppiness, that cause large, unpredictable steps. Even if the steps are controlled by only taking a fraction of the full Gauss-Newton step, the method will rarely converge. Often the fitting processes produces poor fits with “evaporated” parameters, i.e. parameter value going to infinity, zero, or

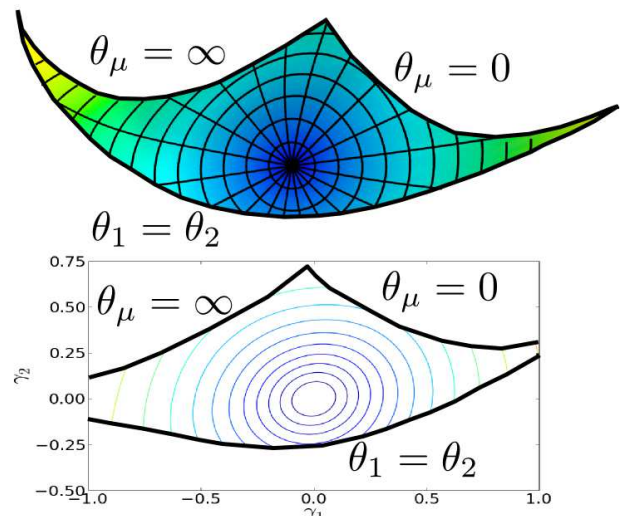


Figure 4: Geodesics can be used to construct a coordinate basis on  $\mathcal{M}$  (above). In these new geodesic coordinates, the cost contours are nearly perfect, isotropic circles (below).

other unphysical values. This failure is understood to be geodesics hitting the boundaries of  $\mathcal{M}$ . The ribbon is nearly flat, but extremely thin. The straight lines of geodesics hit the edges long before finding a good fit.

To improve convergence, we can modify the model manifold to remove the boundaries. One method of doing this is to introduce the *model graph*  $\mathcal{G}$ , which is the parametric surface drawn by the model in data space crossed with parameter space. The metric for the model graph is an interpolation of the data space and parameter space metric,  $g_{\mu\nu} = g_{\mu\nu}^0 + \lambda I_{\mu\nu}$ , where  $\lambda$  determines the weight of the two spaces. Notice that the eigendirections of the metric are the same on both  $\mathcal{M}$  and  $\mathcal{G}$ , however, the eigenvalues on the graph are given by  $\lambda_{\mathcal{G}} = \lambda_{\mathcal{M}} + \lambda$ . Therefore, the sloppy directions with  $\lambda_{\mathcal{M}} \ll \lambda$  have eigenvalues  $\lambda_{\mathcal{G}} \approx \lambda$  on the model graph. By an appropriate choice of  $\lambda$ , we can effectively cut off any of the sloppy eigenvalues of the Hessian. The analogy of the Gauss-Newton step on the model graph is the well-known Levenberg-Marquardt step,  $\delta\theta = -(J^T J + \lambda I)^{-1} \nabla C$  in our notation [8, 9]. By dynamically adjusting the damping parameter,  $\lambda$ , the algorithm can shorten its step and remove the danger of the sloppy directions.

The superiority of the Levenberg-Marquardt algorithm over its Gauss-Newton analog is due the fact that as  $\lambda$  is varied, the direction of the step is rotated from the Gauss-Newton direction into the steepest descents direction. Geometrically we understand the improvement to be due to the lack of boundaries of the model graph. Since most boundaries occur at infinite values of the parameters, the model graph  $\mathcal{G}$  stretches these boundaries to infinity in the parameter space portion of the embedding. (The model graph does not remove boundaries at non-infinite parameter values. It is, therefore, helpful to use parameters for which all boundaries occur at infin-

ity. If the parameters are, for example, rate constants that must be positive, working in log-rates is effective.) In spite of these precautions, the Levenberg-Marquardt algorithm may still evaporate parameters. In these cases it can be helpful to add priors that keep parameters away from unphysical boundaries.

Using the striking simplicity of the cost in geodesic coordinates, we make further improvements to the standard Levenberg-Marquardt algorithm. Interpreting the Levenberg-Marquardt step as a velocity,  $v^\mu = -g^{\mu\nu}\nabla_\nu C$ , where  $g$  is the metric on the model graph, the geodesic acceleration is given by  $a^\mu = -g^{\mu\nu}\partial_\nu\vec{r}\cdot\partial_\alpha\partial_\beta\vec{r}v^\alpha v^\beta$ , giving a step  $\delta\theta^\mu = v^\mu + \frac{1}{2}a^\mu$ .

The geodesic acceleration is very cheap to calculate, requiring only a directional second derivative, which can be estimated from three (cheap) function evaluations (one or two additional function evaluations) at each step with no extra (expensive) Jacobians. The geodesic acceleration serves two purposes. First, it provides an estimate for the trust region in which the linearization approximation (from which Levenberg-Marquardt is traditionally derived) is valid. At each step, the damping term  $\lambda$  should be adjusted until the second order contribution is less than first order contribution. We find that this criterion is more effective than simply tuning until a downhill step is found [9] or considering the reduction ratio [8].

The second benefit of the acceleration occurs when the algorithm must follow a long narrow canyon to the best fit. In these scenarios convergence may be very slow, and approximating the path by a parabola instead of a line can significantly speed up the algorithm. We have observed the number of steps to convergence reduced by a factor of 3 to 10 on moderately sized problems trapped in canyons [10]. (Controlled uphill moves can also speed convergence in these cases [10]).

Just as the special form of the cost function gives an approximate Hessian using only first derivatives of the residuals,  $H \approx J^T J$ , the acceleration has allowed us

to approximate the *cubic* correction using only a directional second derivative. All other algorithms that seek to improve the Levenberg-Marquardt algorithm use second derivative information only to calculate the correction  $\delta H_{\mu\nu} = \vec{r}\cdot\partial_\mu\partial_\nu\vec{r}$ , to the Hessian [11, 12, 13, 14]. This correction is negligible if the nonlinearities are primarily parameter effects curvature; since the unfit data is nearly perpendicular to the surface of the model manifold while the nonlinearities are tangent to the model manifold, the dot product vanishes. Qualitatively, this means that the Gauss-Newton approximate Hessian is very accurate and that the bending of the local ellipses, (due to the third order terms in the cost that we consider), are the leading correction.

By interpreting the fitting process as a generalized interpolation scheme, we have seen that the difficulties in fitting are due to the narrow boundaries on the model manifold,  $\mathcal{M}$ . These boundaries tend to form a hierarchy of widths which are dual to the hierarchy of Hessian eigenvalues characteristic of sloppy models. Additionally, we both observe and argue that the model manifold is remarkably flat (low extrinsic curvature), which leads us to the use of geodesics in the fitting process. The modified Gauss-Newton and Levenberg-Marquardt algorithms are understood to be Euler approximations to the geodesic equation on the model manifold and model graph respectively. By adding a geodesic acceleration to the Levenberg-Marquardt step, we can improve convergence by providing a more accurate trust region, as well as an algorithm more adept at navigating narrow valleys towards the best fit. Given the universality of sloppy models, we expect the geodesic acceleration to be applicable to a wide range of problems.

The authors thank Joshua Waterfall, Chris Myers, Ryan Gutenkunst, John Guckenheimer, and Eric Siggia for helpful discussions. This work was supported by NSF grant number DMR-0705167.

- 
- [1] J. Stoer, R. Bulirsch, W. Gautschi, C. Witzgall: *Introduction to numerical analysis*: Springer Verlag (2002)
  - [2] K. Brown, C. Hill, G. Calero, C. Myers, K. Lee, J. Sethna, R. Cerione: *Physical biology* **1** (2004) 184
  - [3] J. Waterfall, F. Casey, R. Gutenkunst, K. Brown, C. Myers, P. Brouwer, V. Elser, J. Sethna: *Physical Review Letters* **97** (2006) 150601
  - [4] R. Gutenkunst, F. Casey, J. Waterfall, C. Myers, J. Sethna: *Annals of the New York Academy of Sciences* **1115** (2007) 203
  - [5] R. Gutenkunst, J. Waterfall, F. Casey, K. Brown, C. Myers, J. Sethna: *PLoS Comput Biol* **3** (2007) e189
  - [6] D. Bates, D. Watts: *Nonlinear Regression Analysis and Its Applications*: John Wiley (1988)
  - [7] C. Misner, K. Thorne, J. Wheeler: *Gravitation*: WH Freeman and Company (1973)
  - [8] J. Mor: *Lecture notes in mathematics* **630** (1977) 105
  - [9] W. Press: *Numerical recipes: the art of scientific computing*: Cambridge University Press (2007)
  - [10] M. K. Transtrum, B. B. Machta, J. P. Sethna: *The geometry of nonlinear least squares with applications to sloppy models and optimization*: In preparation
  - [11] J. Dennis Jr, J. Moré: *Siam Review* **19** (1977) 46
  - [12] P. Gill, W. Murray: *SIAM Journal on Numerical Analysis* (1978) 977
  - [13] J. Dennis Jr, D. Gay, R. Walsh: *ACM Transactions on Mathematical Software (TOMS)* **7** (1981) 348
  - [14] R. Gonin, S. Toit: *Communications in Statistics-Theory and Methods* **16** (1987) 969